# Time-reversal symmetry breaking in the superconducting state of ScS

Arushi, R. K. Kushwaha, D. Singh, A. D. Hillier, M. S. Scheurer, and R. P. Singh

Letter

# Time-reversal symmetry breaking in the superconducting state of ScS

Arushi,[1] R. K. Kushwaha,[1] D. Singh,[2] A. D. Hillier,[2] M. S. Scheurer [ ],[3] and R. P. Singh [ ][1,*]

[1]*Department of Physics, Indian Institute of Science Education and Research Bhopal, Bhopal 462066, India*
[2]*ISIS Facility, STFC Rutherford Appleton Laboratory, Didcot OX11 0QX, United Kingdom*
[3]*Institute for Theoretical Physics, University of Innsbruck, A-6020 Innsbruck, Austria*

We have studied the electronic properties of ScS, a transition-metal monochalcogenide with a rocksalt crystal structure, using magnetization, specific heat, transport, and muon spin rotation/relaxation ($\mu$SR) measurements. All measurements confirm the bulk superconductivity in ScS with a transition temperature of $T_C = 5.1(5)$ K. Specific heat together with transverse-field $\mu$SR measurements indicate a full gap, while our zero-field $\mu$SR study reveals the presence of spontaneous static or quasistatic magnetic fields emerging when entering the superconducting state. We discuss various possible microscopic origins of the observed time-reversal symmetry breaking. As none of them can be readily reconciled with a conventional pairing mechanism, this introduces ScS as a candidate material for unconventional superconductivity.

The study of unconventional superconductors [1], which go beyond the BCS theory, is a crucial pillar of modern condensed-matter research and involves a broad range of material classes, ranging from heavy fermion systems [2], high $T_C$ superconductors [3,4], to iron-based systems [5,6], and more recently moiré superlattices [7], just to name a few. This research is driven by the potential of these phases for applications and by fundamental scientific questions, such as understanding their pairing mechanism, identifying unifying physical similarities across chemically rather different sets of materials, and finding ways to probe their microscopic physics.

However, even the identification of unconventional pairing is a challenging endeavor: While the presence of nodes in the gap function, which can be protected by symmetry in an unconventional state, is a good indication for unconventional pairing, there are also more subtle unconventional pairing states with a full and approximately isotropic gap [1]. In this case, phase-sensitive techniques are required, with one example given by studying the disorder sensitivity of the pairing state [8–11]. Another phase-sensitive identification is the observation of spontaneous internal magnetic fields at the superconducting transition, indicating that the superconducting order parameter breaks time-reversal symmetry [12–15]. Time-reversal symmetry-breaking superconductivity is particularly interesting since it is rare in nature, the underlying pairing mechanism must involve more than the conventional electron-phonon coupling [16], and due to its potential for technological applications, e.g., for the stabilization of topological edge modes [17], and possibly also for the realization [18,19] of zero-field superconducting diodes [20].

Binary transition-metal arsenides (TMAs) where TM represents a transition metal and A can be any element from the carbon, pnictogen, or chalcogen group, have been widely studied as they provide an exciting family of candidate materials where a range of exotic features has been observed over the years. For instance, NbC, TaC, MoC, VC, and CrC [21–23] exhibit superconductivity together with a nontrivial topological band structure. These compounds crystallize in a centrosymmetric cubic structure known as the rocksalt structure. Motivated by the interest in and exciting properties of these materials, we study ScS, which is isostructural to the above-mentioned compounds.

In this Letter, we report the macroscopic and microscopic study of superconducting properties in ScS by means of magnetization, resistivity, specific heat, and muon spin rotation and relaxation ($\mu$SR) measurements. Superconductivity in ScS has been known for a long time [24,25]; however, a detailed study of the superconducting properties has not yet been performed. All of our measurements confirm bulk superconductivity with a transition temperature of 5.1(5) K. Transverse-field (TF) $\mu$SR indicates a nodeless, approximately isotropic superconducting gap structure together with a slightly enhanced gap to critical temperature ratio compared to the weak-coupling BCS theory. Zero-field (ZF)-$\mu$SR measurements reveal time-reversal symmetry breaking on entering the superconducting state which makes ScS a member of the rocksalt family exhibiting this exotic feature.

*Thermodynamics and transport.* A polycrystalline sample of ScS was prepared by arc melting both the constituent elements on a water-cooled copper hearth under an argon gas atmosphere. To get structural information, powder x-ray diffraction (XRD) on well-grounded powder was performed at 300 K using a PANalytical diffractometer equipped with Cu $K\alpha$ radiation ($\lambda = 1.5406$ Å). ScS adopts a cubic (NaCl defect) crystal structure [see the inset of Fig. 1(a)], with space group $Fm\bar{3}m$ (No. 225), which was determined by the Rietveld refinement of room-temperature powder XRD data shown in the main panel of Fig. 1(a). The lattice
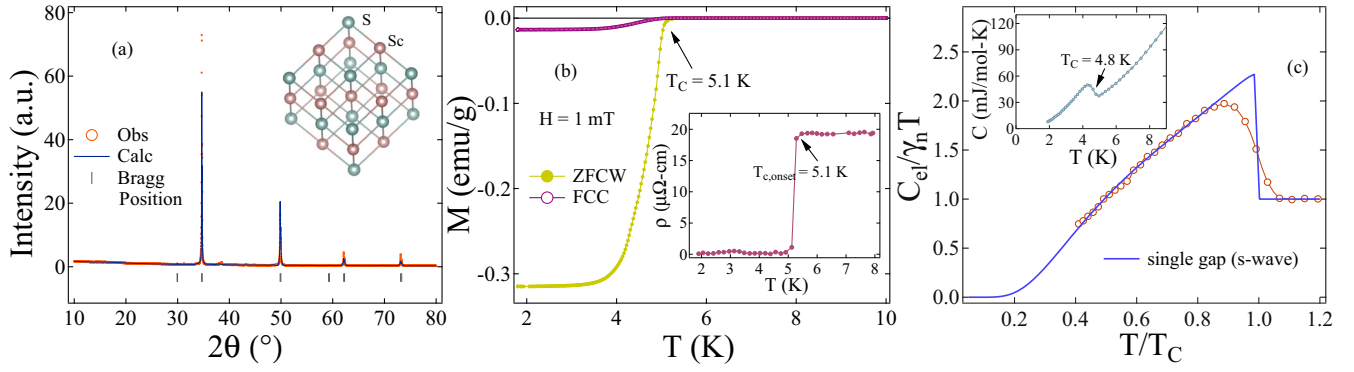
FIG. 1. (a) Powder XRD of ScS obtained at room temperature, shown by open red circles. The solid blue line is the Rietveld refinement whereas the black bars show Bragg reflection peaks. Inset: Crystal structure of ScS. (b) Temperature dependence of the magnetic moment shows $T_C$ at 5.1 K for ScS. The data were collected in an applied field of 1 mT via ZFCW and FCC protocols. The inset shows the enlarged view of the $\rho(T)$ data, with superconducting transition at $T_{C,\text{onset}} = 5.1(2)$ K. (c) Normalized specific heat $C_{\text{el}}/\gamma_n T$ is fitted using a single-gap $s$-wave model represented by the solid blue line. Inset: Temperature dependence of the total specific heat in zero field exhibiting $T_C$ at 4.8(1) K.

constant is $a = 5.172(3)$ Å [see Supplemental Material (SM) [26] Sec. (a)]. To perform magnetization, electrical resistivity, and specific heat measurements, a superconducting quantum interference device (SQUID) (MPMS 3, Quantum Design) and physical property measurement system (PPMS) were used.

Magnetization $M$ measurements collected in an applied field of 1 mT via zero-field cooled warming (ZFCW) and field cooled cooling (FCC) modes confirmed the bulk nature of superconductivity in ScS. As can be seen in Fig. 1(b), it exhibits a diamagnetic signal at a superconducting transition temperature of $T_{C,\text{onset}} = 5.10(5)$ K, where the electrical resistivity data also shows a zero drop in resistivity [inset of Fig. 1(b)]. The difference between the diamagnetic signal in FCC and ZFCW indicates the type II nature of superconductivity in ScS. We extract a Meissner superconducting volume fraction close to 100% from the magnetization measurement. Using $M$ versus field $H$ ($M$ vs $T$) curves at different temperatures (fields) and employing the Ginzburg-Landau relations provided in SM [26] Sec. (c), we obtained the lower and upper critical field as $H_{C1}(0) = 21.0(2)$ mT and $H_{C2}(0) = 0.44(1)$ T. Two important length scales, the penetration depth $\lambda_{\text{GL}}(0)$ and coherence length $\xi_{\text{GL}}(0)$, are found to be 1077(6) and 274(3) Å, respectively. The Ginzburg-Landau parameter $\kappa_{\text{GL}} = \lambda_{\text{GL}}(0)/\xi_{\text{GL}}(0) = 4(1)$ indicates type II superconductivity in ScS. Specific heat measurements at zero field confirmed bulk superconductivity by exhibiting a jump at $T_C = 4.8(1)$ K, which is shown in the inset of Fig. 1(c). From the total specific heat, the electronic specific heat $C_{\text{el}}$ can be calculated by subtracting the phononic contribution [see SM [26] Sec. (d)]; its temperature dependence is shown in the main panel of Fig. 1(c). The dimensionless value of electronic specific heat jump at $T_C$, $\frac{\Delta C_{\text{el}}}{\gamma_n T_C} = 1.13$, is lower than the weak-coupling BCS result (1.43). The temperature dependence of the specific heat below $T_C$ follows more closely a nodeless, isotropic superconducting gap model [see the fit in Fig. 1(c)], yielding $\Delta(0)/k_B T_C = 1.65$, than a nodal $p$-wave or $d$-wave model shown in SM [26] Sec. (d). To estimate the underlying coupling strength $\lambda_M$ of superconductivity, we employed the McMillan model [27] and find $\lambda_M = 0.61(5)$ [SM [26]

Sec. (d)], which indicates moderately coupled pairing in ScS. Also taking into account the measured residual resistance, we extract a ratio of BCS coherence length and mean free path of $\xi_0/l_e = 13.13$ [individual parameter calculations are provided in SM [26] Sec. (d)], signaling dirty limit superconductivity. Details regarding all the calculated parameters employing magnetization, electrical resistivity, and specific heat measurements, as well as the fitting relations, are presented in Secs. (a)–(d) of the SM [26].

*μSR measurements*. Muon spin rotation/relaxation experiments were performed at the ISIS Neutron and Muon facility at the Rutherford Appleton Laboratory, U.K., using a MuSR spectrometer with 64 detectors in both transverse and longitudinal directions. A full description of the muon technique is provided in Ref. [28]. TF-$\mu$SR measurements were carried out in FCC mode where the sample was cooled below the transition temperature (to 0.3 K) in the presence of an external magnetic field. The applied magnetic field was well above the lower critical field [$H_{C1}(0) = 21.0(2)$ mT, SM [26] Sec. (c)] and far below the upper critical critical field which stabilizes the flux line lattice in the mixed superconducting state. Figure 2(a) shows the asymmetry spectra both above and below the transition temperature. The spectra at 0.3 K exhibit a faster relaxation rate than those at 6.5 K, which is due to the inhomogeneous magnetic field distribution from the flux line lattice. The field distribution in the vortex state at 0.3 and 6.5 K using the maximum entropy algorithm (MaxEnt) is shown in Fig. 2(b). At 0.3 K ($T < T_C$), there are two peaks present where one peak corresponds to the applied field sensed by the muons stopping in the sample holder and the other one represents the field distribution due to the flux lattice formation. At $T = 6.5$ K, only one peak is present at the applied field since ScS is in the normal state. The time domain spectra were best modeled by a sinusoidal oscillating function with a Gaussian relaxation plus a sinusoidal oscillation term for muons hitting the sample holder [29,30],

$$A(t) = A_1 \exp\left(-\tfrac{1}{2}\sigma^2 t^2\right) \cos(\gamma_\mu B_1 t + \phi)$$
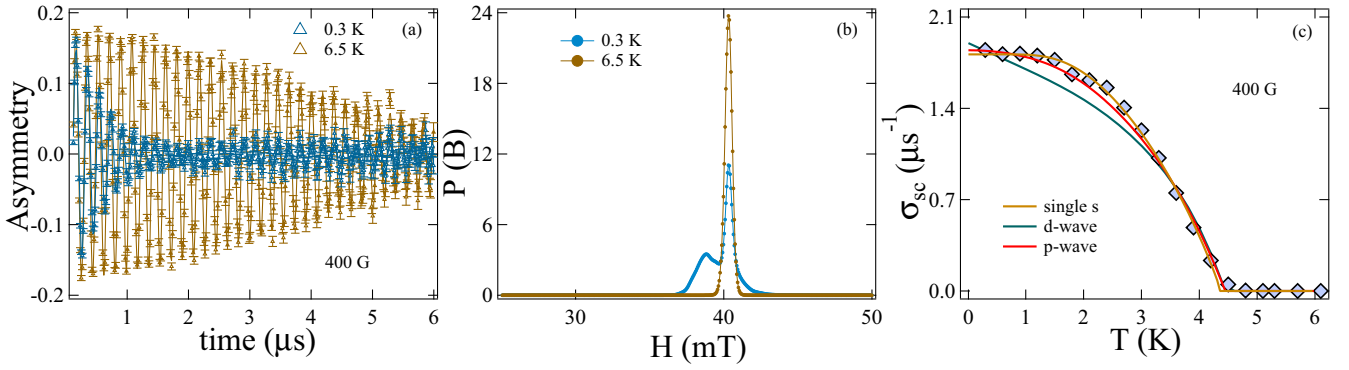$$+ A_{\text{bg}} \cos(\gamma_\mu B_{\text{bg}} t + \phi), \qquad (1)$$

FIG. 2. (a) Transverse-field time domain spectra collected at 6.5 and 0.3 K in an applied magnetic field of 40 mT. The solid lines are fits using Eq. (1). (b) Probability distribution of magnetic field for $T < T_C$ and $T > T_C$. (c) Temperature dependence of $\sigma_{sc}$ (squares), where solid lines represent fitting using Eq. (2) which employs $s$-, $p$-, and $d$-wave models.

where $A_1$, $B_1$, and $\sigma$ are the initial asymmetry, internal field, and the Gaussian muon spin relaxation rate belonging to the sample. $\gamma_\mu/2\pi = 135.5$ MHz/T is the muon gyromagnetic ratio. $A_{bg}$ and $B_{bg}$ are the asymmetry and field contributions coming from the background when muons hit the sample holder. The relaxation rate corresponding to the superconducting contribution $\sigma_{sc}$ can be calculated after subtracting the nuclear magnetic dipolar contribution $\sigma_{ndip}$ using the following expression, $\sigma_{sc} = \sqrt{\sigma^2 - \sigma_{ndip}^2}$ , where $\sigma_{ndip}$ is assumed to be constant over the entire temperature range; the resulting temperature dependence of $\sigma_{sc}$ is shown in Fig. 2(c). Since $\sigma_{sc}$ is related to the magnetic penetration depth as $\sigma_{sc} \propto \lambda^{-2}$, it contains information about the form of the superconducting gap structure. Assuming a single, spherical Fermi surface, it holds [31–33]

$$\frac{\sigma_{sc}(T)}{\sigma_{sc}(0)} = 1 + 2\left\langle \int_{|\Delta(T,\hat{k})|}^{\infty} \frac{\partial f}{\partial E} \frac{E\,dE}{\sqrt{E^2 - \Delta^2(T,\hat{k})}} \right\rangle. \quad (2)$$

Here, $f = [\exp(E/k_B T) + 1]^{-1}$ is the Fermi-Dirac function and $\langle \cdot \rangle$ represents the average over the Fermi surface. $\Delta(T,\hat{k}) = \Delta_0(T)g_{\hat{k}}$ is the temperature ($T$) and the directional ($\hat{k}$)-dependent superconducting gap. Using spherical coordinates with angles $\phi$ and $\theta$, we will consider the cases $g_{\hat{k}} = 1$, $|\sin(\theta)|$, and $|\cos(2\phi)|$ for a fully gapped $s$-wave, $p$-wave with nodal points, and $d$-wave state with nodal lines, respectively. The temperature dependence of the gap function is approximated by $\Delta_0(T) \simeq \Delta_0(0)\tanh\{1.82[1.018(t^{-1} - 1)]^{0.51}\}$, where $\Delta_0(0)$ is the magnitude of the superconducting gap at zero temperature. As can be seen in Fig. 2(c), the data are best captured by the fully gapped $s$-wave model, providing the value of the superconducting gap $\Delta(0)/k_B T_C = 2.0$ which is slightly greater than the gap value estimated from the specific heat (1.65) as well as the standard BCS gap value (1.76), but not inconsistent with the moderately weak-coupling constant $\lambda_M \simeq 0.6$ extracted above [34]. A small discrepancy between the gap magnitudes obtained from the specific heat and $\mu$SR studies may be due to the lack of specific heat data at low temperatures. To fully understand the gap nature in ScS, further work will be needed such as a detailed study on the Fermi surface of ScS.

To search for the possible magnetism (static or fluctuating) in ScS, we have performed ZF-$\mu$SR measurements as

this technique is extremely sensitive to tiny magnetic fields associated with TRS-breaking phases; these measurements were performed in the presence of an active compensation system in order to cancel the stray magnetic field within the range of 0.01 G. The time domain spectra were taken above (8.0 K) and below (0.3 K) the transition temperature $T_C$ as shown in Fig. 3(a). There is a significant difference in the relaxation rate observed across $T_C$, hinting towards the spontaneous emergence of magnetic fields in the superconducting state. For nonmagnetic samples, the depolarization can be best described with the function given below,

$$A(t) = A_0 G_{KT}(t)\exp(-\Lambda t) + A_1, \quad (3)$$

where $\Lambda$ is the Lorentzian relaxation component, $A_1$ is the flat background, $A_0$ is the asymmetry signal coming from the sample; furthermore, $G_{KT}$ is the static Kubo-Toyabe function provided as [35]

$$G_{KT}(t) = \frac{1}{3} + \frac{2}{3}(1 - \Delta^2 t^2)\exp\left(\frac{-\Delta^2 t^2}{2}\right), \quad (4)$$

with $\Delta$ representing the Gaussian muon spin depolarization rate which accounts for the randomly oriented, static nuclear moments experienced at the muon site. The rise in the extracted $\Lambda(T)$ [see Fig. 3(b)] in the superconducting state confirms the presence of spontaneous magnetic fields. To exclude the possibility of an impurity-induced relaxation, we have performed an additional longitudinal measurement at 0.3 K. A magnetic field of 30 mT was sufficient to decouple the muon spins from the internal magnetic field [Fig. 3(a)]. It suggests the presence of a static or quasistatic magnetic field.

*Discussion.* Taken together, our measurements of specific heat and penetration depth point towards a fully developed nodeless superconducting gap, while our zero-field $\mu$SR data indicate the emergence of weak magnetic moments below a temperature very close to the superconducting $T_C$. To explore the implications for the superconducting state in ScS, we will next discuss and critically evaluating four possible microscopic origins, labeled as scenarios (i)–(iv) below, of this phenomenology.

In *scenario (i)*, we assume that the superconducting phase is reached by a single-phase transition, which is natural as
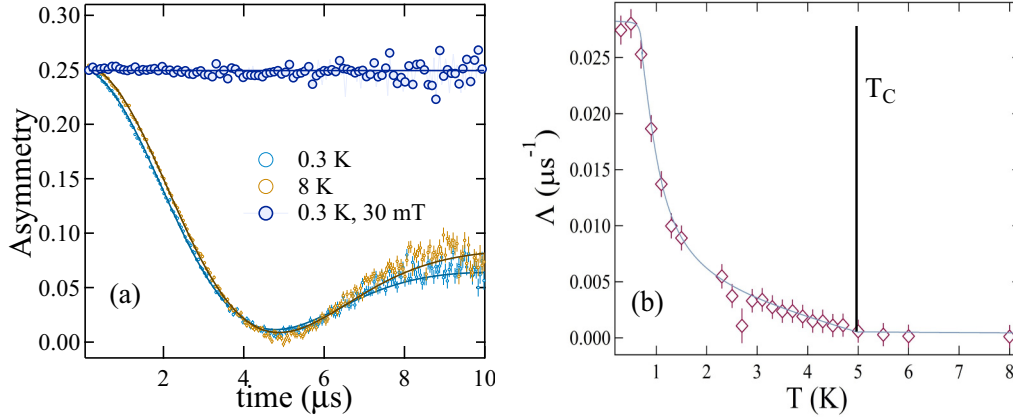
FIG. 3. (a) Asymmetry spectra recorded at two different temperatures, 0.3 and 8.0 K, in zero magnetic field (small open circles); data at a small longitudinal field (30 mT) are shown by large solid circles. The solid lines are the corresponding fits to the data using Eq. (3). (b) shows the temperature dependence of the relaxation rate $\Lambda$ with a guide to the eye line, featuring an increase below the superconducting transition temperature $T_C$.

there are no indications of multiple superconducting transitions. The order parameter must then transform under one of the (ten) irreducible representations (IRs) of the normal-state point group $O_h$. We further assume that the observed magnetic moments result from the time-reversal symmetry breaking of the superconducting state itself. As is well known, this is only possible if it transforms under a two- or higher-dimensional IR—in our case, one of the six IRs $E_g$, $T_{1g}$, $T_{2g}$, $E_u$, $T_{1u}$, $T_{2u}$, leading to a total of ten possible time-reversal symmetry-breaking candidate states [1]. All of them are required by symmetry to have at least one nodal direction (in some cases even nodal planes) around the $\Gamma$ point. However, first-principles calculations [36] predict two Fermi surfaces enclosing the $\Gamma$ point completely, such that any of these superconductors is expected to have nodes. While this seems to be at odds with our specific heat and penetration depth data, it is possible that these nodes are not resolved in our measurements. The reason might be the disorder present in the polycrystalline compound which can suppress the nodes in the superconducting gap due to significant scattering. As such, we believe that specific heat measurements at lower temperature or more accurate penetration depth studies, e.g., using the tunnel diode resonator technique [37] on a single crystal of ScS, might help decide whether or not this scenario is realized.

Another possibility, *scenario (ii)*, to reconcile broken time-reversal symmetry and a full gap is based on having two consecutive superconducting transitions that are so close that they cannot be resolved. When the dominant repulsive Cooper-channel interactions are *between* the three symmetry-unrelated Fermi sheets of the system, a natural compromise in this "frustrated" situation might be to have nontrivial complex phases of the order parameter between these sheets and a fully gapped $s + is$ state might be realized (see, e.g., the toy model discussion in Ref. [38] or the mechanism for time-reversal symmetry-breaking superconductivity in the iron-based superconductors [39,40]); such a state will give rise to magnetic moments [41] that can be detected by the muons. Note, however, that by virtue of transforming under the trivial (and thus

one-dimensional) IR of $O_h$, such a state can only be reached by two, possibly very close, phase transitions. We hope that future high-quality crystals will exhibit a sharper phase transition signature in the specific heat, possibly allowing us to confirm or rule out this scenario.

One additional complication for both of these scenarios is that we have estimated the coherence length $\xi_0$ to be larger than the mean free path $l_e$, indicating a significant amount of disorder in the superconductor. Therefore, common wisdom [42,43] would imply that any of the aforementioned unconventional superconducting states should be completely suppressed by impurity scattering. However, a more recent theory [44–48] has reveal that spin-orbit coupling can protect unconventional pairing states, which is also supported by experiment [49–51]. Moreover, disorder can even be the driving force inducing a time-reversal symmetry-breaking superconductor, which leads us to *scenario (iii)*: As demonstrated in recent theoretical works on $d$-wave superconductors [52,53], when two superconducting pairing channels are in close competition, strong disorder can locally induce complex admixtures of these orders leading to local currents, even if the clean sample was in a time-reversal symmetric state. Finally, as pointed out in Ref. [54], in a granular sample such as the one studied here, a single sign-changing superconducting order parameter can give rise to flux trapping in voids formed by three or more crystallites, defining *scenario (iv)*.

Importantly, all of these scenarios, (i)–(iv), require effectively repulsive Cooper-channel interactions, at least for parts of the Fermi surface, and thus necessitate [16,55] an unconventional pairing mechanism in the sense that the pairing state cannot be understood in terms of electron-phonon coupling alone. The only conceivable picture to explain our observations with a conventional pairing mechanism requires assuming that there are local magnetic moments that are strongly screened in the normal state. At the onset of superconductivity, this screening might be reduced and could lead to the enhancement of the relaxation rate in Fig. 3(b) below $T_C$; this was recently proposed [56] for $4Hb$-TaS$_2$ where signs of Kondo screening have been observed [57]. However, for

ScS, we did not find any signs of screening of magnetic moments nor are we aware of any signs reported in the literature, ruling out this scenario.

*Conclusion and outlook*. We have presented transport, magnetization, specific heat, and $\mu$SR experiments in the superconducting and normal state of ScS, which crystallizes in a rocksalt (NaCl) structure. All measurements confirmed the bulk nature of superconductivity, with a transition temperature $T_C = 5.1(5)$ K. We extracted various superconducting and normal-state parameters of ScS. Specific heat data and the temperature dependence of the penetration depth following from TF-$\mu$SR measurements are most naturally explained by a fully established superconducting gap. Surprisingly, our zero-field $\mu$SR data reveal time-reversal symmetry-breaking moments at the onset of superconductivity. We have discussed several possible microscopic origins of these moments, which suggest that the underlying pairing glue cannot arise solely from the electron-phonon coupling, but rather requires repulsive components. As such, our results establish

ScS as a system exhibiting complex superconducting properties that deserve further investigation. In particular, $\mu$SR measurements in high-quality single crystals, specific heat measurements at low temperatures, as well as complementary penetration depth measurements [37] and controlled disorder studies should be able to elucidate the microscopics of superconductivity in ScS.

[1] M. Sigrist and K. Ueda, Rev. Mod. Phys. **63**, 239 (1991).

[2] B. D. White, J. D. Thompson, and M. B. Maple, Physica C: Supercond. **514**, 246 (2015).

[3] D. J. Van Harlingen, Rev. Mod. Phys. **67**, 515 (1995).

[4] S. Sachdev, Rev. Mod. Phys. **75**, 913 (2003).

[5] F. Wang and D.-H. Lee, Science **332**, 200 (2011).

[6] J. Liu, P. Dai, D. Feng, T. Xiang, and F.-C. Zhang, Nat. Sci. Rev. **1**, 3 (2014).

[7] Y. Cao, V. Fatemi, S. Fang, K. Watanabe, T. Taniguchi, E. Kaxiras, and P. Jarillo-Herrero, Nature (London) **556**, 43 (2018).

[8] A. P. Mackenzie, R. K. W. Haselwimmer, A. W. Tyler, G. G. Lonzarich, Y. Mori, S. Nishizaki, and Y. Maeno, Phys. Rev. Lett. **80**, 161 (1998).

[9] F. Rullier-Albenque, H. Alloul, and R. Tourbot, Phys. Rev. Lett. **91**, 047001 (2003).

[10] J. Li, Y. Guo, S. Zhang, S. Yu, Y. Tsujimoto, H. Kontani, K. Yamaura, and E. Takayama-Muromachi, Phys. Rev. B **84**, 020513(R) (2011).

[11] E. H. Krenkel, M. A. Tanatar, M. Konczykowski, R. Grasset, E. I. Timmons, S. Ghimire, K. R. Joshi, Y. Lee, Liqin Ke, S. Chen, C. Petrovic, P. P. Orth, M. S. Scheurer, and R. Prozorov, Phys. Rev. B **105**, 094521 (2022).

[12] G. M. Luke, Y. Fudamoto, K. M. Kojima, M. I. Larkin, J. Merrin, B. Nachumi, Y. J. Uemura, Y. Maeno, Z. Q. Mao, Y. Mori, H. Nakamura, and M. Sigrist, Nature (London) **394**, 558 (1998).

[13] G. M. Luke, A. Keren, L. P. Le, W. D. Wu, Y. J. Uemura, D. A. Bonn, L. Taillefer, and J. D. Garrett, Phys. Rev. Lett. **71**, 1466 (1993).

[14] Y. Aoki, A. Tsuchiya, T. Kanayama, S. R. Saha, H. Sugawara, H. Sato, W. Higemoto, A. Koda, K. Ohishi, K. Nishiyama, and R. Kadono, Phys. Rev. Lett. **91**, 067003 (2003).

[15] G. M. Luke, Y. Fudamoto, K. M. Kojima, M. I. Larkin, B. Nachumi, Y. J. Uemura, J. E. Sonier, Y. Maeno, Z. Q. Mao, Y. Mori, and D. F. Agterberg, Physica B: Condens. Matter **289-290**, 373 (2000).

[16] M. S. Scheurer, Phys. Rev. B **93**, 174509 (2016).

[17] J. Alicea, Rep. Prog. Phys. **75**, 076501 (2012).

[18] B. Zinkl, K. Hamamoto, and M. Sigrist, arXiv:2111.05340.

[19] H. D. Scammell, J. I. A. Li, and M. S. Scheurer, 2D Mater. **9**, 025027 (2022).

[20] J.-X. Lin, P. Siriviboon, H. D. Scammell, S. Liu, D. Rhodes, K. Watanabe, T. Taniguchi, J. Hone, M. S. Scheurer, and J. I. A. Li, arXiv:2112.07841.

[21] T. Shang, J. Z. Zhao, D. J. Gawryluk, M. Shi, M. Medarde, E. Pomjakushina, and T. Shiroka, Phys. Rev. B **101**, 214518 (2020).

[22] R. Zhan and X. Luo, J. Appl. Phys. **125**, 053903 (2019).

[23] A. Huang, A. D. Smith, M. Schwinn, Q. Lu, T. R. Chang, W. Xie, H. T. Jeng, and G. Bian, Phys. Rev. Materials **2**, 054205 (2018).

[24] A. R. Moodenbaugh, D. C. Johnston, and R. Viswanathan, Mater. Res. Bull. **9**, 1671 (1974).

[25] A. R. Moodenbaugh, D. C. Johnston, R. Viswanathan, R. N. Shelton, L. E. DeLong, and W. A. Fertig, J. Low Temp. Phys. **33**, 175 (1978).

[26] See Supplemental Material at http://link.aps.org/supplemental/10.1103/PhysRevB.106.L020504 for the comprehensive calculation of various superconducting and normal state parameters, which includes Refs. [27,58–71].

[27] W. L. McMillan, Phys. Rev. **167**, 331 (1968).

[28] A. D. Hillier, S. J. Blundell, I. McKenzie, I. Umegaki, L. Shu, J. A. Wright, T. Prokscha, F. Bert, K. Shimomura, A. Berlie, H. Alberto, and I. Watanabe, Nat. Rev. Methods Primers **2**, 4 (2022)

[29] M. Weber, A. Amato, F. N. Gygax, A. Schenck, H. Maletta, V. N. Duginov, V. G. Grebinnik, A. B. Lazarev, V. G. Olshevsky, V. Yu. Pomjakushin, S. N. Shilov, V. A. Zhukov, B. F. Kirillov, A. V. Pirogov, A. N. Ponomarev, V. G. Storchak, S. Kapusta, and J. Bock, Phys. Rev. B **48**, 13022 (1993).

[30] A. Maisuradze, R. Khasanov, A. Shengelaya, and H. Keller, J. Phys.: Condens. Matter **21**, 075701 (2009).

[31] B. S. Chandrasekhar and D. Einzel, Ann. Phys. **505**, 535 (1993).

[32] R. Prozorov and R. W. Giannetta, Supercond. Sci. Technol. **19**, R41 (2006).

[33] D. T. Adroja, A. Bhattacharyya, M. Telling, Y. Feng, M. Smidman, B. Pan, J. Zhao, A. D. Hillier, F. L. Pratt, and A. M. Strydom, Phys. Rev. B **92**, 134505 (2015).

[34] R. Combescot and G. Varelogiannis, Solid State Commun. **93**, 113 (1995).

[35] R. S. Hayano, Y. J. Uemura, J. Imazato, N. Nishida, T. Yamazaki, and R. Kubo, Phys. Rev. B **20**, 850 (1979).

[36] D. Shrivastava and S. P. Sanyal, Comput. Condens. Matter **21**, e00418 (2019).

[37] C. T. Van Degrift, Rev. Sci. Instrum. **46**, 599 (1975).

[38] Arushi, D. Singh, A. D. Hillier, M. S. Scheurer, and R. P. Singh, Phys. Rev. B **103**, 174502 (2021).

[39] S. Maiti and A. V. Chubukov, Phys. Rev. B **87**, 144511 (2013).

[40] V. Grinenko, R. Sarkar, K. Kihou, C. H. Lee, I. Morozov, S. Aswartham, B. Büchner, P. Chekhonin, W. Skrotzki, K. Nenkov, R. Hühne, K. Nielsch, S.-L. Drechsler, V. L. Vadimov, M. A. Silaev, P. A. Volkov, I. Eremin, H. Luetkens, and H.-H. Klauss, Nat. Phys. **16**, 789 (2020).

[41] J. Garaud and E. Babaev, Phys. Rev. Lett. **112**, 017003 (2014).

[42] R. Balian and N. R. Werthamer, Phys. Rev. **131**, 1553 (1963).

[43] A. A. Golubov and I. I. Mazin, Phys. Rev. B **55**, 15146 (1997).

[44] K. Michaeli and L. Fu, Phys. Rev. Lett. **109**, 187003 (2012).

[45] M. S. Scheurer, M. Hoyer, and J. Schmalian, Phys. Rev. B **92**, 014518 (2015).

[46] D. C. Cavanagh and P. M. R. Brydon, Phys. Rev. B **101**, 054509 (2020).

[47] E. I. Timmons, S. Teknowijoyo, M. Konczykowski, O. Cavani, M. A. Tanatar, S. Ghimire, K. Cho, Y. Lee, L. Ke, N. H. Jo, S. L. Bud'ko, P. C. Canfield, P. P. Orth, M. S. Scheurer, and R. Prozorov, Phys. Rev. Research **2**, 023140 (2020).

[48] D. Dentelski, V. Kozii, and J. Ruhman, Phys. Rev. Research **2**, 033302 (2020).

[49] M. Kriener, K. Segawa, S. Sasaki, and Y. Ando, Phys. Rev. B **86**, 180505(R) (2012).

[50] S. Sasaki, K. Segawa, and Y. Ando, Phys. Rev. B **90**, 220504(R) (2014).

[51] M. P. Smylie, K. Willa, H. Claus, A. Snezhko, I. Martin, W.-K. Kwok, Y. Qiu, Y. S. Hor, E. Bokari, P. Niraula, A. Kayani, V. Mishra, and U. Welp, Phys. Rev. B **96**, 115145 (2017).

[52] C. N. Breiø, P. J. Hirschfeld, and B. M. Andersen, Phys. Rev. B **105**, 014504 (2022).

[53] Z. X. Li, S. A. Kivelson, and D. H. Lee, npj Quantum Mater. **6**, 36 (2021).

[54] P. K. Biswas, H. Luetkens, T. Neupert, T. Stürzer, C. Baines, G. Pascua, A. P. Schnyder, M. H. Fischer, J. Goryo, M. R. Lees, H. Maeter, F. Brückner, H.-H. Klauss, M. Nicklas, P. J. Baker, A. D. Hillier, M. Sigrist, A. Amato, and D. Johrendt, Phys. Rev. B **87**, 180503(R) (2013).

[55] P. M. R. Brydon, S. Das Sarma, H.-Y. Hui, and J. D. Sau, Phys. Rev. B **90**, 184512 (2014).

[56] D. Dentelski, E. Day-Roberts, T. Birol, R. M. Fernandes, and J. Ruhman, Phys. Rev. B **103**, 224522 (2021).

[57] W. Ruan, Y. Chen, S. Tang, J. Hwang, H.-Z. Tsai, R. L. Lee, M. Wu, H. Ryu, S. Kahn, F. Liou, C. Jia, A. Aikawa, C. Hwang, F. Wang, Y. Choi, S. G. Louie, P. A. Lee, Z.-X. Shen, S.-K. Mo, and M. F. Crommie, Nat. Phys. **17**, 1154 (2021).

[58] G. Grimvall, *The Electron-Phonon Interaction in Metals* (North-Holland, Amsterdam, 1981).

[59] A. Bid, A. Bora, and A. K. Raychaudhuri, Phys. Rev. B **74**, 035426 (2006).

[60] E. Helfand and N. R. Werthamer, Phys. Rev. **147**, 288 (1966).

[61] N. R. Werthamer, E. Helfand, and P. C. Hohenberg, Phys. Rev. **147**, 295 (1966).

[62] A. B. Karki, Y. M. Xiong, I. Vekhter, D. Browne, P. W. Adams, D. P. Young, K. R. Thomas, J. Y. Chan, H. Kim, and R. Prozorov, Phys. Rev. B **82**, 064512 (2010).

[63] J. K. Bao, J. Y. Liu, C. W. Ma, Z. H. Meng, Z. T. Tang, Y. L. Sun, H. F. Zhai, H. Jiang, H. Bai, C. M. Feng, Z. A. Xu, and G. H. Cao, Phys. Rev. X **5**, 011013 (2015).

[64] K. Maki, Phys. Rev. **148**, 362 (1966).

[65] M. Tinkham, *Introduction to Superconductivity*, 2nd ed. (McGraw-Hill, New York, 1996).

[66] T. Klimczuk, F. Ronning, V. Sidorov, R. J. Cava, and J. D. Thompson, Phys. Rev. Lett. **99**, 257004 (2007).

[67] C. B. Vining, R. N. Shelton, H. F. Braun, and M. Pelizzone, Phys. Rev. B **27**, 2800 (1983).

[68] O. J. Taylor, A. Carrington, and J. A. Schlueter, Phys. Rev. Lett. **99**, 057001 (2007).

[69] X. Xu, B. Chen, W. H. Jiao, Bin Chen, C. Q. Niu, Y. K. Li, J. H. Yang, A. F. Bangura, Q. L. Ye, C. Cao, J. H. Dai, G. Cao, and N. E. Hussey, Phys. Rev. B **87**, 224507 (2013).

[70] C. Q. Niu, J. H. Yang, Y. K. Li, B. Chen, N. Zhou, J. Chen, L. L. Jiang, B. Chen, X. X. Yang, C. Cao, J. Dai, and X. Xu, Phys. Rev. B **88**, 104507 (2013).

[71] A. Carrington and F. Manzano, Physica C: Supercond. **385**, 205 (2003).